# STRUCTURE LIGHT SYSTEM APPLIED TO 3D SURFACE DEFECTS INSPECTION

Ma Zongzheng[1], Ma Haishu[1], Yu Quan[2], Yan Xiupeng[1]

*Surface defect is one of the most common defects of industry product. Sometimes the defect feature such as depth and length could be used to determine whether it is a defective product. In order to ensure the high quality of products and reduce the manufacturing costs, the three-dimensional (3D) inspection is needed. So one 3D surface defect inspection system focusing on hole defect based on structured light system (SLS) is developed. The system consists of two parts: hardware and software. The hardware includes camera and projector which are controlled by the computer. The software can realize point cloud input, point cloud segment, hole number determination, and hole feature extraction which is programmed on MATLAB. First the system is validated using holes on a wood plane board. Then it is used to inspect the holes feature on a connecting rod surface and this method can measure the hole diameter about 1mm and achieves high measurement accuracy. Finally, some effects on measurement accuracy are discussed, such as external light and surface reflection.*

**Keywords**: Surface defect; Feature extraction; Inspection; SLS; 3D.

## 1. Introduction

In order to ensure the high quality of products and reduce the manufacturing costs, product surface inspection has always been deemed as the crucial part in manufacturing industries. The detection of defects such as dents or cracks is the main purpose in quality inspection. It is especially challenging to localize the small defects on a large area surface [1, 2]. Human inspection is subjected to the

[1]Dept. of Mechanical Engineering, Henan University of Engineering, China,
e-mail: zongzhengma@haue.edu.cn
[2]Dept. of Production and Quality Engineering, Norwegian University of Science and Engineering, Norway

limitations such as low speed, accuracy and reliability due to boredom and fatigue [3-5].Therefore, the technologies to realize the automation of quality inspection are greatly needed.

Early inspection methods relied on the analysis of digital images to recognize the defects. In [6, 7] convolutional neural networks are trained on the database of images of steel surface for defect detection. Thresholding method is employed in [8] for detection of defects on high resolution images of titanium-coated aluminum specimens. However, the main restriction of image based inspection is the lack of 3D information such as the shape of the product and the depth of the defects [9, 10]. Coordinate measuring machine is widely used for quality inspection, which utilizes the touching probe to obtain the 3D point data of the product [11]. But as a contact method, the scanning speed of Coordinate Measuring Machine (CMM) is extremely low and it is very likely to cause scratch in the product [12].

The recent development of structured light vision provides an alternative to address this problem. By projecting a known pattern on the surface of the product, the structured light system (SLS) can extract the depth and surface information from the object [13]. Moreover, the SLS is cost effective because only camera and projector are needed in the system. Many researches have been conducted based on the SLS technology. [14] presents a new automated 3D vision quality inspection system which combines SLS and data mining approaches together. 3D coordinate information is acquired from SLS. Features are extracted from the point cloud data for defect classification. An original framework for the detection of defects on an airplane exterior surface is proposed in [15], which analyzes the 3D data collected with the 3D structured light scanner. Structured light system has been applied for welding inspection [16]. The proposed method extracts metric information about the thickness and angle deformation of the welds from the 3D model obtained with SLS. However, there are no researches that identify the number and feature extraction of defects on the product surface based on the analysis of the point clouds acquired from the SLS.

In this paper we propose a robust approach to detect the defects of the product based on SLS. Firstly, the principle and components of SLS are introduced. Then the hardware selection and corresponding software development of the 3D surface defect inspection system are finished. After the validation of the system based on wood plane holes, it is applied to find the number of the defects and their

dimensions, depths and orientations of a connecting rod. Finally, some effects on measurement accuracy are discussed, such as external light and surface reflection.

The rest of the paper is organized as follows: section II introduces the principle of SLS, section III presents the SLS system, the hardware configuration of SLS and the 3D defect inspection software development are introduced in section IV and section V, section VI gives the application of the measurement system, section VII presents some effects on measurement, finally the conclusions are given.

## 2. Principle of SLS

According to the depth information retrieving methods, the SLS can be divided into three main categories, i.e. time of flight (ToF) methods, interferometry methods and triangulation methods. Most of the applications are based on triangulation principle or interferometry. Due to the involving of the light source and coded pattern projection, the depth information is able to be recovered by analyzing the deformation of the patterns. Hardware of a typical SLS consists of a digital camera (CMOS or CCD) as the imaging device, a digital projector (LED or DLP) to project light patterns, and a computer to do the image analysis as shown in Fig.1.

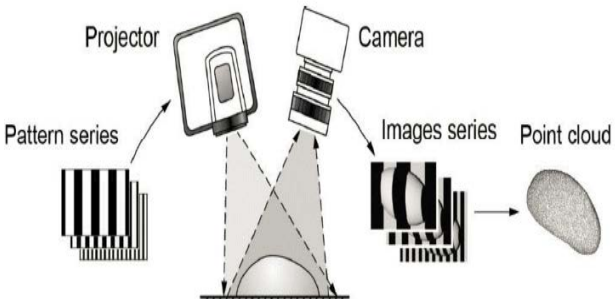


Fig. 1. Structured light system

In SLS, the scene is illuminated by fringe range contours with a light source passing through a grating. While the scene image is captured by a displaced camera through an identical second grating. The resulting interference pattern shows equidistant contour lines, which can be converted into range information. In a structured light system, the coded pattern includes time-series of codes or color codes.

The mathematical model of the SLS is based on the triangulation as shown in Fig.2.

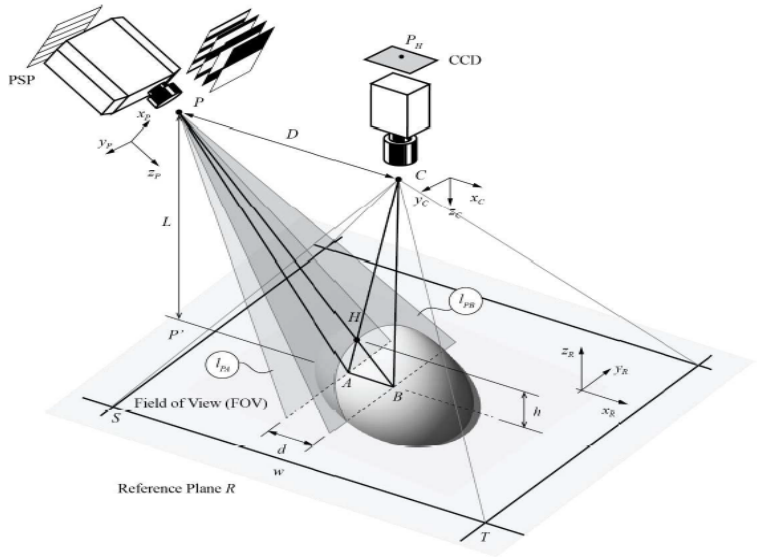


Fig. 2. Optical geometry of the SLS

Points P and C represent the exit and the entrance pupils of the projection and imaging optics, respectively, D is the distance between them, and L is the distance the from plane R. The coordinate system at the Projection Sensor Plane (PSP) is (XP, YP, ZP) and that of the imaging plane in camera (CCD) is (XC, YC, ZC) . The origins are at points P and C, respectively. Axes ZP and ZC coincide with the optical axes of the projection and the imaging devices: ZC is perpendicular to reference R, and ZP is at an angle with respect to ZC.

The depth information is defined along the ZR coordinate in the reference system (XR, YR, ZR). The discrete coordinates at the CCD are j and k, corresponding respectively to XC and YC. is the width of the field of view along the coordinate.

Because the fringes formed at the PSP are parallel to YP, when the YP coordinate varies, different light planes can be identified: As an example, Fig.2 shows two light planes, denoted by lPA and lPB, defined in correspondence to two different values of coordinate XP . In the figure, light ray PA on lPA is also depicted: It intersects plane R at point A and is imaged by pixel Px(j,k) at the CCD. Axes YP, YC, and YR are all parallel to each other: Thus, the measuring procedure does not involve them and in the following they are not considered. Considering triangles ΔAHB and ΔPHC are similar, the height of point H can be calculated by

$$\mathrm{h} = Ld / (D + d) \tag{1}$$

Where L and D are respectively the distance from P to reference R and from P to C, and d is the distance between A and B computed as

$$d = X_B - X_A \tag{2}$$

## 3. SLS System introduction

A SLS can be considered as a point cloud acquisition system using camera devices and projected light patterns, which is used for the three dimensional shape measurement of an object. A structured light system includes two parts of hardware and software, respectively. As shown in Fig.3, the hardware comprises a control unit (generally a PC), a light source (a laser emitter or a projector) and image acquisition devices (one or more cameras). While the software module commonly includes SLS calibration module, the pattern projecting module, the image acquisition module and the point cloud extraction module.

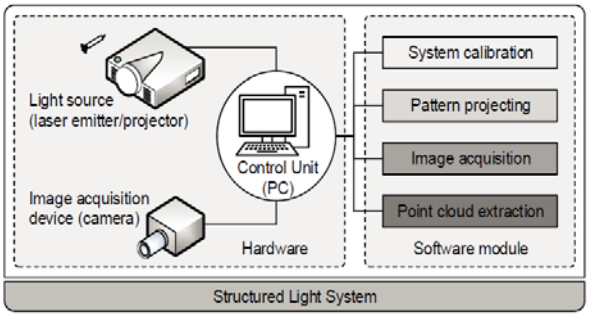


Fig. 3. Diagram of SLS system

The function of each component is briefly described below:

The control unit (PC) controls the light source and image acquisition devices, and receives the image obtained from the image acquisition devices. Moreover, the control unit extracts point cloud from obtained images using programs stored on it.

The light source is employed to project some specific light patterns onto the scene, in other words, to encode the scene with the light patterns. Commonly used light source includes laser emitter and projector.

The image acquisition device is used to capture the scene images with CMOS/CCD sensor. According to the specific algorithm of point cloud construction, one or more cameras are set as the image acquisition devices.

The system calibration module aims to obtain the system parameters of the SLS, which includes both intrinsic and extrinsic parameters. This parameter acquisition process is also known as calibration. The SLS is unavailable to use until the calibration is performed.

The pattern projecting module and image acquisition module are commonly performed together. The pattern projecting module is used to project a light pattern or pattern series onto the scene so that the scene is encoded with the patterns, meanwhile the image acquisition module controls the camera to obtain the scene image or image series sequentially if using pattern series.

The point cloud extraction module works based on obtained scene images, the encoding principle of the projected light patterns and the system parameters retrieved from calibration module. Point cloud of the scene is extracted by analyzing the real-time scene images. The point set of inspected product is also available to be separated according to some filtering rules.

The following parts will introduce the hardware configuration and software development.

## 4. Hardware configuration of SLS

The hardware of SLS is composed of camera and projector. The selection of camera and projector is discussed in this part.

*A. Camera selection*

The principle of camera can be seen as convex lens imaging and the principle of the convex lens imaging is shown in Fig 4. The model can be also viewed as the pinhole camera model if only considering the optical center while ignoring the shape of the convex lens.

The back focal distance means the distance between the lens and the focal plane, which is larger than the focal length. The focal length here is to be calculated as

$$L_f = \frac{d \times l}{l_0 + l} \tag{3}$$

Where $d$ denotes the working distance, $l$ denotes the CCD length, $l_0$ is the object size. The steps of camera and lens selection include that:

*1) Determining the Field of View (FOV)*

Apparently, the size of the FOV should be larger than the object that is to be inspected, in order to cover the whole part.

According to actual size of this measurement system the FOV is 500mm× 500mm.

*2) Determining the working distance*

In practical, the working distance is the distance between the object and the lens' leading edge, which is used to avoid interfering(Fig.5). For this measurement system the working distance is 1100mm.

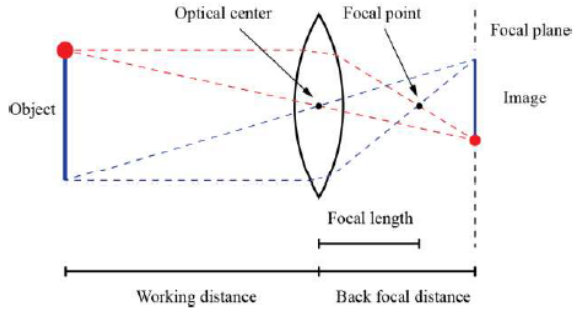


Fig.4. The simplified convex lens imaging model

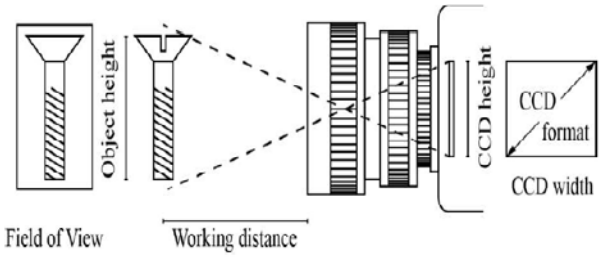


Fig.5. The camera model in practical application

*3) Calculating the focal length*

It shows a simple lens model in Fig. 4. Two focal lengths are calculated with respective to the width $l_w$ and height $l_h$ of the CCD, and the chosen lens format should be smaller than the smaller one.

The two focal lengths are calculated as

$$L_{fw} = \frac{d \times l_w}{l_0 + l_w} = \frac{1100 \times 7.2}{500 + 7.2} = 15.6mm \tag{4}$$

$$L_{fh} = \frac{d \times l_h}{l_0 + l_h} = \frac{1100 \times 5.4}{500 + 5.4} = 11.7mm \tag{5}$$

According to actual size of this measurement system the Pentax h1214-M lens is used with 1/3" format.

*4) Determining the view orientation and the size of the CCD*

It is a good way to use a suitable view orientation to take a good advantage of the camera. The format of CCD chips and lenses is based on the films and tube cameras in olden times, which is listed in Table 1. The format of CCD should be less than or equal to that of the lens.

*Table 1*

**CCD FORMAT**

| CCD format | Hight/mm | Width/mm |
|---|---|---|
| 1/4" | 2.4 | 3.2 |
| 1/3" | 3.6 | 4.8 |
| 1/2" | 4.8 | 6.4 |
| 1/1.8" | 5.4 | 7.2 |
| 1" | 9.6 | 12.8 |

Based on the lens used in this measurement system, the SONY XCG-U100E model CCD camera is used with a 1/1.8"format and1600 mm×1200mm resolution.

*B. Selection of the projector*

Considering the working distance was short in this measurement system the short focal length projector BENQ-MW632ST was used.Then the parameters and type of equipment used in this system are list in Table 2.

*Table 2*

**The parameters and type of equipment**

| Equipment | Type | Parameters |
|---|---|---|
| Projector | BENQMW632ST | Minimum projection distance:625mm; projection area:862x538mm |
| CCD camera | SONY XCG-U100E | format:1/1.8"; Pixels:1600 x 1200 |
| Lens | Pentax h1214-M | Screen size:1/3", Front focal length:12 mm ±5%;Back focal length:11.50 mm |

## 5. Three-Dimensional defect inspection software development

The software includes the calibration module, pattern projecting module, image acquisition module, and point cloud extraction module. The calibration module, pattern projecting module, and image acquisition module are completed by Scorpion Vision Software from Tordivel. Therefore, only the 3D defect inspection module should be developed based on the MATLAB platform.

The main difficulty in 3D defect inspection is how to determine the number of defects and defect feature extraction. So the hole defect is selected in this paper and the following analysis is based on hole defect inspection.

*A. Points Cloud input*

There are many data formats that can be read in MATLAB. The point cloud data format collected in this measurement system is .csv whose data volume is large. So the csvread() command is used to read in the MATLAB and the point cloud data is stored in a M matrix using specific command M = csvread('image.csv').

*B. Point cloud segment*

In order to detect the hole feature, the hole's point cloud should be obtained firstly. So the point cloud segment is done based on the point cloud matrix M read into the MATLAB.

Since the hole studied has certain depth even though it is not a through hole and the Z value of the corresponding point is different from the surface points, the Z value can be used to segment point cloud. Notably the Z value represents the value of depth direction of the hole.

It also should be noted that, due to the influence of external light sources and projectors, the obtained Z values of the surface points are not exactly the same and it varies within an range. Therefore, an interval range is used to distinguish the point cloud that is the surface or the hole.

*C. Determination of the number of holes*

Before determining the characteristics of a hole, it is necessary to determine how many holes in the part. Here, the k-menas function is used which can calculate the sum of distance (sumD) from each point to its centroid.

[Idx,C,sumD,D]=Kmeans(X,K, 'Param1',Val1) returns distances from each point to every centroid in the n-by-k matrix D. Where the C is the centroid locations and returned as a numeric matrix, sumD is sums of point-to-centroid distances, D is the distances from each point to every centroid, the X is the data, the K is the number of clusters in the data, Param1 is the option parameters which is selected as Distance in this paper, Val1 is the corresponding value of Param1 and the Squared Euclidean distance is used.

Assuming that the number of the holes in the point cloud is K, so the number of centroid is K and the point cloud is divided into K sections. When the K is smaller than the actual number of holes, the sumD is very big since the centroid is not

correct. Then the sumD will decrease rapidly when the K is equal to or bigger than the real number of holes. Based on this, the K value can be obtained by using the loop method, and K represents the number of holes.

*D. Hole Feature Extraction and Display*

For a hole defect, general features include position, diameter, and hole depth. For the diameter, the maximum distance of two points at XY plane is considered as the hole diameter using the Matlab's inherent function ‘pdist’ to calculate the point cloud data for each hole. The center position of the hole is represented by the XY coordinates of the point whose Z value is the smallest among all the data of the hole. The depth of the hole is obtained by the Z value difference between the XY plane and the point which has the smallest Z value.

At the end of the flowchart, matching based inspection and measuring based inspection are applied respectively for the recognized segments, according to the 3D shape inspection rules that are predefined.

## 6. Application of the measurement system

The measurement system is applied to a connecting rod which is shown in Fig. 6. There are two different holes in the crank connecting rod surface drilled before the test. Then the two holes features are extracted with the measurement system.

Fig.6. Connecting rod for test

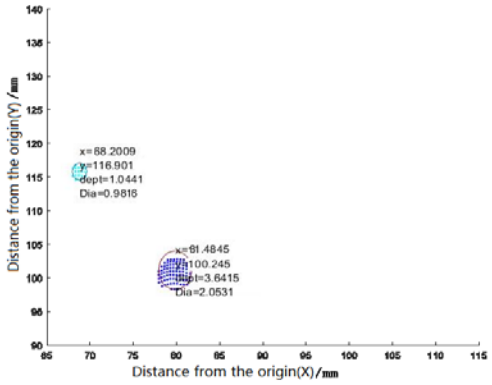


Fig.7. Feature of extracted from point cloud

Fig.7 shows the extracted feature of two holes on the surface where the x and y represent the hole center coordinates, the depth of the hole represented by dep1, Dia represents the diameter of the hole. Notably, the coordinates zero is

defined as the lower-left corner of the picture. The big hole depth is 3.6415 mm, and the diameter is 2.1931 mm, while the small hole depth is 1.2442 mm, and the diameter is 1.241 mm. From above test, this system can extract the hole feature and show it with vivid way. It also shows that this method can measure the diameter of about 1mm hole and has certain degree of measurement accuracy.

## 7. Some effects of measurement

It also should be noted that there are results error because of external light, reflection, and CCD camera. So the effects of these on measurement results are studied.

*A. The effects of light on measurement*

Fig. 8 shows the comparison of plane point cloud with and without external light. When there is an external light source, the measured Z value of the surface varies from 9.5mm to 11.8mm which is obviously not suitable for the practical application. When there is no external light source, the measured Z value difference is less than 1mm.

As mentioned before, the measurement method is based on gray codes which mainly depend on the gray value. If there is an external light source beside the projector, the obtained gray value will be large. So it is necessary to consider the influence of external light sources in practical applications and a darkroom is an option.

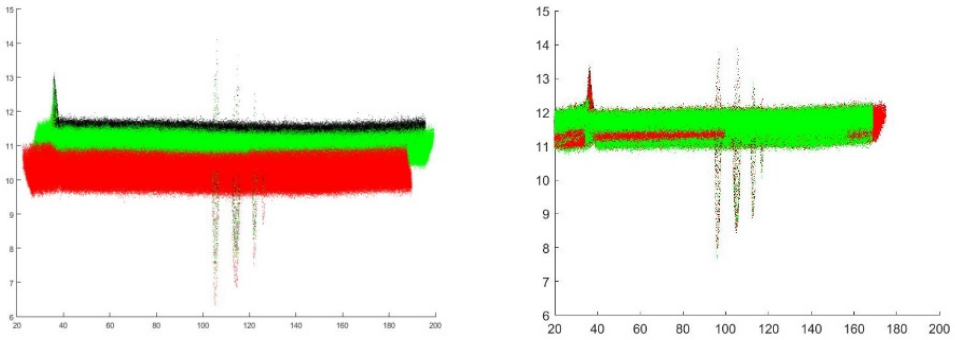


(a)With external light (b)Without external light

Fig.8. Effect of external light on point cloud

### *B. The effects of reflection on measurement*

(a)Connecting rod without coating

(b) Connecting rod with coating

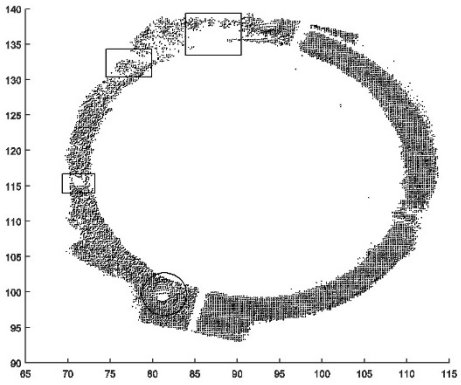


(c) Acquired point cloud without coating

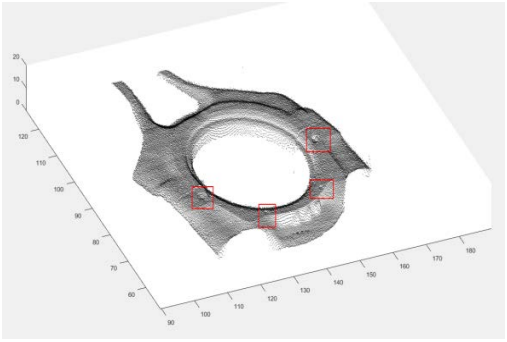

(d)Acquired point cloud with coating

Fig.9 Effect of reflection on point cloud

Fig.9 shows the metal surface point clouds comparison with and without coating. It shows that when there is no coating, it is hard to acquire hole feature because the reflection of the metal is serious. In contrast, when there is coating, the collected point cloud data is more complete, and it is easy to acquire hole feature. In the actual application, the coating on the metal surface is needed which can change the reflection to diffuse reflection and facilitate the extraction process.

## 8. Conclusion

In order to extract surface defect 3D feature an approach for 3D surface defects inspection measurement based on structured light is developed. The following conclusions are derived from the investigations.

(1) Based on convex lens imaging model, the working distance, lens, and CCD camera can be determined when the FOV and the focal length are calculated.

The projector can also be determined considering the working distance and focal length.

(2) The program based on MATLAB platform can extract the hole feature based on the processing of point cloud input, point cloud segment, hole number determination, and hole feature extraction and display.

(3) When the system is applied to a connecting rod surface hole defect inspection, the results show that this system can retrieve the hole feature and show it with vivid way and its measured minimum hole diameter can be around 1mm.

(4) The system can be affected by external light and surface reflection, which can lead to Z value error more than 2mm and the hole feature is hard to retrieve when the metal surface has no coating because of the reflection. The alternative method is to place a polarizing filter in front of the camera lens to suppress the reflections.

**Acknowledgement**

This work was supported by Young key teachers Supporting Project of Henan Province (2014GGJ S-120). The authors would like to express appreciation for financial support from the Reliability Engineering Center of Henan Institute of Engineering and the Power-driven Machinery and Vehicle Engineering Research Center of Henan Institute of Engineering.

## R E F E R E N C E S

[1] *S. Sharifzadeh, I. Biro, N. Lohse, and P. Kinnell,* "Abnormality detection strategies for surface inspection using robot mounted laser scanners," Mechatronics, vol. 51, pp. 59-74, 2018.

[2] *D. Kang, Y. J. Jang, and S. Won,* "Development of an inspection system for planar steel surface using multispectral photometric stereo," Optical Engineering, vol. 52, no. 3, pp. 039701, 2013.

[3] *M.-K. Kim, J. C. Cheng, H. Sohn, and C.-C. Chang,* "A framework for dimensional and surface quality assessment of precast concrete elements using BIM and 3D laser scanning," Automation in Construction, vol. 49, pp. 225-238, 2015.

[4] *J.-K. Park, B.-K. Kwon, J.-H. Park, and D.-J. Kang,* "Machine learning-based imaging system for surface defect inspection," International Journal of Precision Engineering and Manufacturing-Green Technology, vol. 3, no. 3, pp. 303-310, 2016.

[5] *A. Barari,* "Inspection of the machined surfaces using manufacturing data," Journal of Manufacturing Systems, vol. 32, no. 1, pp. 107-113, 2013.

[6] *D. Soukup, and R. Huber-Mörk*, "Convolutional neural networks for steel surface defect detection from photometric stereo images." pp. 668-677.

[7] *J. Masci, U. Meier, D. Ciresan, J. Schmidhuber, and G. Fricout*, "Steel defect classification with max-pooling convolutional neural networks." pp. 1-6.

[8] *M. Win, A. Bushroa, M. Hassan, N. Hilman, and A. Ide-Ektessabi*, "A Contrast Adjustment Thresholding Method for Surface Defect Detection Based on Mesoscopy," IEEE Trans. Industrial Informatics, vol. 11, no. 3, pp. 642-649, 2015.

[9] *L. Li, Z. Wang, F. Pei, and X. Wang*, "Improved illumination for vision-based defect inspection of highly reflective metal surface," Chinese Optics Letters, vol. 11, no. 2, pp. 021102, 2013.

[10] *C. Koch, K. Georgieva, V. Kasireddy, B. Akinci, and P. Fieguth*, "A review on computer vision based defect detection and condition assessment of concrete and asphalt civil infrastructure," Advanced Engineering Informatics, vol. 29, no. 2, pp. 196-210, 2015.

[11] *N. Audfray, C. Mehdi-Souzani, and C. Lartigue*, "A novel approach for 3d part inspection using laser-plane sensors," Procedia CIRP, vol. 10, pp. 23-29, 2013.

[12] *P. Hong-Seok, and T. U. Mani*, "Development of an inspection system for defect detection in pressed parts using laser scanned data," Procedia Engineering, vol. 69, pp. 931-936, 2014.

[13] *H. Radvar-Esfahlan, and S.-A. Tahan*, "Robust generalized numerical inspection fixture for the metrology of compliant mechanical parts," The International Journal of Advanced Manufacturing Technology, vol. 70, no. 5-8, pp. 1101-1112, 2014.

[14] *Y. Li, C. Liu, J. X. Gao, and W. Shen*, "An integrated feature-based dynamic control system for on-line machining, inspection and monitoring," Integrated Computer-Aided Engineering, vol. 22, no. 2, pp. 187-200, 2015.

[15] *K.-S. Wang*, "Towards zero-defect manufacturing (ZDM)—a data mining approach," Advances in Manufacturing, vol. 1, no. 1, pp. 62-74, 2013.

[16] *Q. Yu, and K. Wang*, "3D vision based quality inspection with computational intelligence," Assembly Automation, vol. 33, no. 3, pp. 240-246, 2013.